VOL.39 Nº3 2022
https://doi.org/10.22230\IMECTA.9237.en

Study of densification and phaseformation of alumina ceramics doped with niobium and lithium fluoride

Pedro Craveiro Rodrigues dos Santos Credmann[a], Pedro Henrique Poubel Mendonça da Silveira[b], Matheus Pereira Ribeiro[c], Thuane Teixeira da Silva[d], Alaelson Vieira Gomes[e]
[a]pedro.craveiro.rodrigues@gmail.com, [b]pedroo.poubel@gmail.com, [c]mpmatheusr@gmail.com, [d]thuaneteixeiraa@gmail.com, [e]alaelson@ime.eb.br

RESUMO: As propriedades das cerâmicas avançadas permitem sua adoção como proteção balística, principalmente naquelas compostas de diversas camadas, presente na primeira camada de impacto. Dentre estas cerâmicas, a alumina (Al2O3) possui menor custo por sua facilidade de obtenção, mas está limitada à baixa flexão e tenacidade à fratura. Desta forma, propõe-se a adoção de aditivos, como a niobia (Nb2O5) e o fluoreto de lítio (LiF), os quais já apresentaram melhorias na sinterização e densificação do material final. O presente trabalho analisou a influência destes compostos na alumina de modo a se observar a formação de fases. Dessa forma, observou-se um incremento de cerca de 14% na densificação. Além disso, constatou-se a ausência de impurezas através da observação das fases no ensaio de DRX. As análises em MEV constatou a diminuição da porosidade e das fases formadas após a sinterização.

PALAVRAS-CHAVE: Densificação. Cerâmicas Avançadas. Alumina. Nióbia. Fluoreto de Lítio.

ABSTRACT: The properties of advanced ceramics allow their adoption as ballistic protection, especially the multilayered, which are in the first impact layer. Among these ceramics, alumina (Al2O3) has a lower cost due to its ease of obtaining, but it is limited to low flexion and fracture toughness. Thus, it is proposed the use of additives, such as niobium oxide (Nb2O5) and lithium fluoride (LiF), which have already shown improvements in the sintering and densification of the final material. The present work analyzed the influence of these compounds on alumina in order to observe the phase formation. There was an increase of about 14% in densification. Furthermore, the absence of impurities was verified through the phases in the XRD test. The SEM analyzes found a decrease in porosity and phases formed after sintering.

KEYWORDS: Densification. Advanced Ceramics. Alumina. Niobium Oxide. Lithium Fluoride.

1. Introduction

Advanced ceramics are widely used as ballistic shielding. This is mainly due to its mechanical properties added to characteristics such as low density, which provide a great mechanical strength/density ratio compared to other classes of materials used for the same purpose. [1-3]

It is possible to apply advanced ceramics in mixed shields, which are composed of overlapping plates of different materials in order to use each of their characteristics to guarantee the best possible performance. As ceramic materials have high hardness and compressive strength, but low tensile strength, they are used in the first layer in order to resist the initial compression events resulting from the impact of the projectile. [4-6]

One of the main ceramics used in the manufacture of shields is aluminum oxide (Al_2O_3), also called alumina. This material is one of the most studied advanced ceramics due to its low cost, ease of obtaining and good mechanical, electrical, thermal and chemical properties. On the other hand, they have application limitations due to low flexural strength and fracture toughness, with their low resistance to thermal shock. [7-9]

In order to reduce the consequences of the aforementioned limitations, some doping elements are inserted in the alumina composition, which generates an improvement in densification, as well as in flexural strength and fracture toughness. [10] One of the elements known to influence the properties of alumina is niobium-niobium oxide (Nb_2O_5). This oxide, when added in small fractions in the alumina composition, presented results that prove the improvement in the original ceramic properties.

Gomes and collaborators [11] added 4 and 6% by weight of Nb2O5 in the alumina composition. In this study there was an increase in densification and a reduction in the sintering temperature from 1600 °C to 1400 °C. Trindade

et al. [12] investigated the influence of sintering time on the densification of alumina ceramics doped with 4% by weight of Nb_2O_5. Thus, it was verified that the increase in the total sintering time has a significant effect on the increase in density.

Another dopant that can be used in conjunction with Nb_2O_5 is lithium fluoride (LiF). When added in small concentrations to alumina with Nb_2O_5, LiF accelerates diffusion during sintering and increases the densification and hardness of alumina ceramics. Some recent works reported the use of LiF as a dopant in the composition of alumina. Santos et al. [13] investigated the influence of adding LiF at concentrations ranging from 0% to 1.5%, together with the addition of 4% Nb_2O_5. In this study it was found that the addition of 0.5% LiF conferred better properties such as greater densification and hardness. Silveira et al. [14] studied the influence of the activation of phases formed by the interaction between Nb_2O_5 and LiF, through calcination of these materials and then added to alumina. Greater densifications were found in groups with calcination temperatures close to the LiF melting temperature.

Thus, the objective of this work is to evaluate the densification of alumina ceramics, doped with niobia and lithium fluoride, and to analyze the formation of phases after sintering.

2. Materials and Methods

2.1 Starting Materials

The powders used for making ceramics are: α-Al_2O_3 APC 11 SG, rom the manufacturer Alcoa (Brazil); Nb_2O_5, acquired by Companhia Brasileira de Metalurgia e Mineração - CBMM (Brazil); lithium fluoride (LiF), obtained by Dinâmica (Brazil). The organic binder used to give resistance to the green body was Polyethylene glycol (PEG 300) from the company Isofar (Brazil).

Next, in **table 1**, the masses used to form the mixture, the density of each item and its percentage in total weight are described.

Tab.1 - Density of the constituent elements of the ceramics produced.

Material	Density (g/cm$^{3)}$
AI_2O_3	3,96
Nb_2O_5	4,60
LiF	2,65
PEG	-

The density of the mixtures was determined from the Rule of Mixtures, given below in **equation 1**, where the densities of each element and their fraction by weight were used, excluding the PEG, eliminated during sintering.

$$\rho = (\rho_{Al2O3} x m_{Al2O3}) + (\rho_{Nb2O5} x m_{Nb2O5}) + (\rho_{LiF} + m_{LiF}) \quad (3)$$

The percentages of addition of each element were 0.5% by weight of LiF, 4% by weight of Nb_2O_5 and 95.5% by weight of Al_2O_3. In **table 2,** the densities of each mixture composition are described.

Tab. 2- Theoretical density of samples obtained using the mixture rule.

Material	Density (g/cm$^{3)}$
AI_2O_3	3,960
AI_2O_3 - 4%pNn2O5	3,985
AI_2O_3 -4%pNb2O5 - 0,5%p LiF	3,979

2.2 Sample Processing

The starting materials were placed in an alumina-lined jar. Next to these elements, deionized water in a 1:1 ratio was inserted, in order to facilitate the homogenization, and alumina balls, for a better comminution of the powders. Grinding and mixing was done in a ball mill for a period of 8 hours, followed by drying in an oven at a temperature of 80 °C for a period of 48 hours.

After drying, the mixture resulting from the milling was deagglomerated with the aid of a pestle and mortar, followed by sieving to obtain the desired granulometry. A sieve shaker was used for a period of 3 min, adopting a DIN 4188 sieve with an opening of 0.255 mm.

The preparation of the green ceramic bodies was done through uniaxial cold pressing by a SKAY press,

with a capacity of 30 t. Ceramic discs were prepared with 15 mm diameter matrices for Archimedes and bending tests. Its pressing was carried out in two stages: the first consisted of a light pre-load for the settlement of the powders in the matrix and the subsequent pressing with a load of 30 MPa in order to give the powders the shape of a tablet.

The sintering process of the samples was carried out conventionally, without controlled presence. Sintering was carried out in a JUNG furnace with the process reaching a maximum temperature of 1400 °C. The sintering route is shown below in **figure 1.**

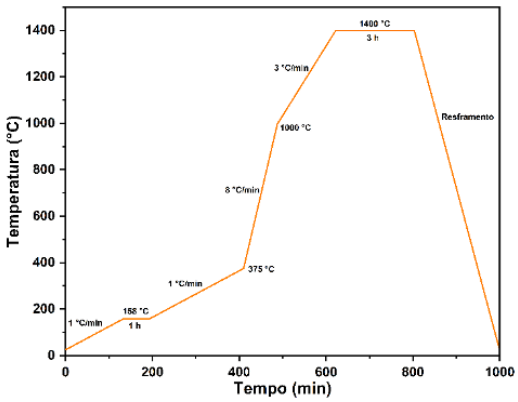

Fig. 1 – Sintering route used in this study.

2.3 Characterization

2.3.1 Green Density Calculation

From the theoretical density value found through the Rule of Mixtures, it was possible to calculate the density and densification of the green ceramic bodies. Thus, **equation 2** was adopted to determine the green density, based on the relationship between mass and volume of the sample. The green densification, shown below in **equation 3**, was calculated from the percentage difference in the density value obtained by the theoretical density found in the mixture rule of **equation 1.**

$$\rho_{verde} = \frac{massa_{amostra}}{volume_{amostra}} \quad (2)$$

$$Densificação_{verde} = (\frac{\rho_{verde}}{\rho_{teórica}})x100\% \quad (3)$$

2.3.2 Densification of Sintered Samples

The calculation of density and densification of the sintered ceramic bodies was performed based on NBR 16667: 2017. [15] Through **equation 4**, based on Archimedes' technique, which considers the data of immersed mass (mi), wet mass (mu) and dry mass (ms), the apparent density is obtained. With this result, it is possible to determine the densification of the ceramic body through the difference between the apparent density and the theoretical density of the body (**equation 5**).

$$\rho_{aparente} = (\frac{m_s}{m_u - m_i})x\rho_{líq} \quad (4)$$

$$Densificação = (\frac{\rho_{aparente}}{\rho_{tteórica}})x100\% \quad (5)$$

2.3.3 X-Ray Diffraction (XRD)

XRD analysis allowed the identification of the phases present in the starting powders and in the sintered samples. The test was carried out in a Panalytical X'pert MRD diffractometer, with Co-Kα radiation, 40 KV power and 30 m current. The sweep ranged from 5 to 80°.

2.3.4 Scanning Electron Microscopy (SEM)

Observation of the fracture surface of the sintered samples was performed using a QUANTA FEG 250 scanning electron microscope. A beam with a power of 20 kV and a diameter of 5 μm was used. Magnifications varied between 2000 and 20,000x, in order to allow microstructures to be examined. Samples were previously coated with gold to allow complete visualization.

3. Results and Discussion

3.1 Densification of Samples

Next, in **table 3**, the green densification results of the analyzed sample groups are described.

Tab. 3- Density results relative to the green of the samples.

Material	Density (g/cm$^{3)}$	Green Densification (%)
Al_2O_3	2,174 ± 0,08	54,53 ± 2.09

Al_2O_3/4%pNb_2O_5	2,506 ± 0,05	62,80 ± 1,17
Al_2O_3/4%pNb_2O_5 /0,5%p LiF	2,322 ± 0,05	58,09 ± 1,42

The result obtained for pure alumina, 54.53%, is compatible with the literature. [16] It is proposed there that, for a good sintering of bodies composed of alumina, the densification of the green bodies must be at least 55%. The addition of niobium to alumina considerably influenced the relative green densification of the ceramic bodies, where an increase in densification to 62.80% was observed. In turn, the addition of LiF exerted a minor influence on the parameter of the analyzed samples.

Next, in **table 4,** the relative density results of the samples after sintering are described.

Tab. 4 - Results of density and relative densification of sintered samples.

Material	Density (g/cm$^{3)}$	Relative Densification (%)
Al_2O_3	3,289 ± 0,067	83,06 ± 1,69
Al_2O_3/4%pNb_2O_5	3,700 ± 0,053	92,84 ± 1,33
Al_2O_3/4%pNb_2O_5 /0,5%p LiF	3,836 ± 0,027	96,41 ± 0,68

From the values displayed in **table 4**, it is possible to observe that the densification of all sample groups presented high values when compared to the literature. Pure alumina showed a densification of 83.06%, a value higher than what Gomes et al. [11] found for the same material sintered at 1600 °C (71.8 %).

The addition of niobium and lithium fluoride caused a relevant increase in the densification of alumina ceramics. The samples with 4% of niobium reached an average densification of 92.84%, while the ceramics with the addition of 4% of niobium and 0.5% of LiF showed a densification of 96.41%. These values are higher than those found in several other studies. [11-14,17,18] The increase in the densification of samples with niobium and lithium fluoride is due to sintering in the liquid phase. In this process, dopants with a low melting point form a eutectic phase that runs through the pores and voids of the ceramic, which facilitates the grain diffusion process and the formation of densification necks. [19]

3.2 X-Ray Diffractometry

Next, **figures 2 and 3** show the diffractograms of the precursor materials used and the sintered ceramics with their respective phases indicated.

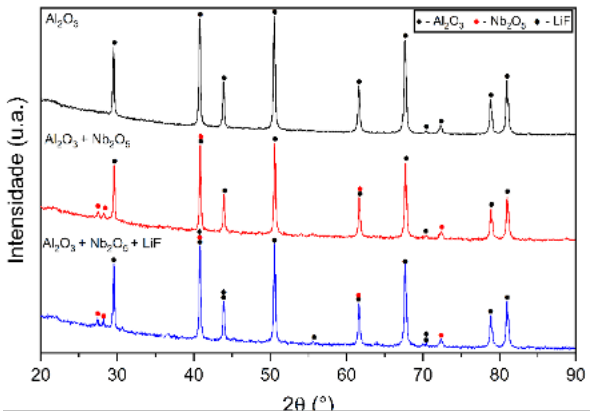

Fig. 2 – Diffractograms of the departure powders.

From the diffractograms in **figure 2**, it is possible to observe that the precursor materials did not present impurities that could harm the densification of the samples. This is justified by the presence of only the phases related to alumina, niobium and lithium fluoride, respectively.

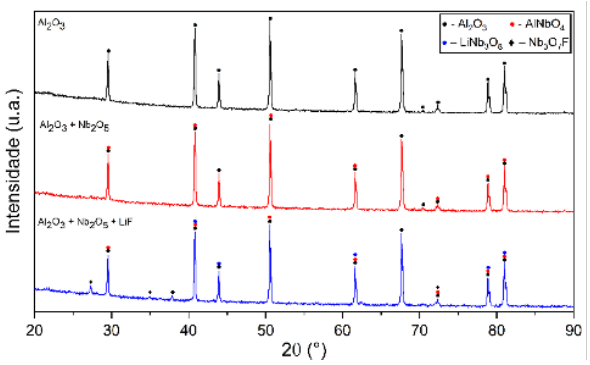

Fig. 3 – Diffractograms of the sintered samples.

From the diffractograms in **figure 3**, it is possible to observe the formation of three phases besides alumina during sintering. The interaction of alumina

with niobia during the homogenization step causes the formation of aluminum niobate ($AlNbO_4$) at high temperatures. [20] In turn, the lithium niobate phase ($LiNbO_3$) is formed from the interaction of niobia at temperatures above 1000 °C, forming a liquid phase. The formation of $LiNbO_3$ promotes increased densification because the liquid phase fills the pores, which contributes to increased diffusion and densification of alumina. [21] The niobium fluoride phase (Nb_3O_7F) was also found in the sintered samples. This phase is formed from the melting temperature of LiF, where the interaction with niobium allows it to disappear completely, leaving only the phases $LiNbO_3$ and Nb_3O_7F. [22]

The presence of these phases is a factor of great importance in controlling the microstructure of alumina, as these phases act directly in accelerating the diffusivity of grain boundaries, promoting greater densification of ceramics. [23] The formation of these phases preferentially in the grain boundaries is the key to the increase in densification, because the fact that the grain boundary is a region of higher energy, the grains tend to grow in these regions. As a result, the total area of the grain boundary decreases, reducing the free energy of the system. [24] The liquid phases precipitated in the grain boundaries block the movement, favoring the elimination of the pores linked to this grain boundary. [24,25]

3.2 Scanning Electron Microscopy (SEM)

Fracture micrographs of the analyzed samples are shown below in **figures 4, 5 and 6. figure 4** shows the alumina fracture surface at 5000x and 20000x magnification.

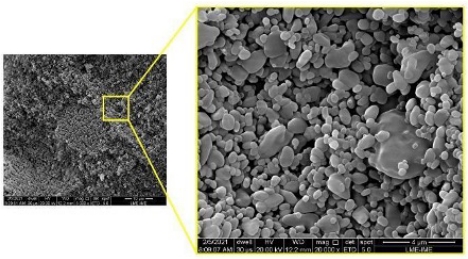

Fig. 4 – Micrographs of the fracture region of the pure alumina sample. 5000 and 20000x magnification.

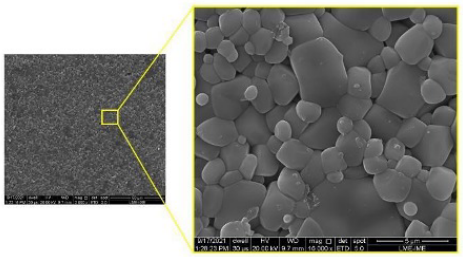

Fig. 5 – Micrographs of the fracture region of the niobia-doped alumina sample. Magnifications of 2000 and 16000x.

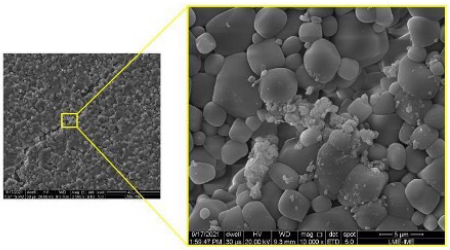

Fig. 6 – Micrographs of the fracture region of the alumina sample doped with niobium and lithium fluoride. Magnifications of 2500 and 10000x.

From the micrographs in **figure 4,** it is possible to observe that the pure alumina samples showed high porosity. This high porosity is due to the lack of dopants in the alumina composition, directly influencing the sintering mode.

The alumina samples doped with niobia showed a considerable increase in densification, which can be observed in the micrograph of **figure 5** and corroborated by the densification results presented in topic 3.2 of this work. The addition of niobium to alumina formed $AlNbO_4$ which is already reported in previous research as a phase that promotes the acceleration of grain diffusion, lodging especially in the grain boundaries, reducing the porosity of the material and promoting an increase in densification. [11-14]

Samples doped with niobia and lithium fluoride showed very high relative densifications, almost reaching 97% densification. In the micrographs of Figure 6, it is possible to observe the formation of intergranular cracks in the sample. These cracks were

specifically concentrated in the grain boundaries, traversing the sample in its entirety. The almost absence of pores is due to the filling of voids by the eutectic phases formed during sintering. ($AlNbO_4$, $LiNbO_3$ and Nb_3O_7F)

6. Conclusions

In this work, advanced alumina ceramics doped with 4% by weight of Nb_2O_5 and 0,5% and 0.5% by weight of LiF were produced through conventional sintering at a temperature of 1400 °C for 3 hours.

The presented results showed that the addition of Nb_2O_5 increased the alumina densification by 14%, due to the formation of liquid phases that favored diffusion during the sintering step of the samples.

Acknowledgements

This work was carried out with the support of the Coordination for the Improvement of Higher Education Personnel Brazil (CAPES) - Financing Code 001.

References

[25] G.J. APPLEBY-THOMAS, D.C. WOOD, A. HAMEED, J. PAINTER, B. FITZMAURICE, On the effects of powder morphology on the post-comminution ballistic strength of ceramics, Int. J. Impact Eng. 100 (2017) 46–55. https://doi.org/10.1016/j.ijimpeng.2016.10.008.

[26] X. GUO, X. SUN, X. TIAN, G.J. WENG, Q.D. OUYANG, L.L. ZHU, Simulation of ballistic performance of a two-layered structure of nanostructured metal and ceramic, Comp. Struct. 157 (2016) 163–173. https://doi.org/10.1016/j.compstruct.2016.08.025.

[27] J. PITTARI, G. SUBHASH, J. ZHENG, V. HALLS, P. JANNOTTI, The rate-dependen fracture toughness of silicon carbide- and boron carbide-based ceramics, J. Eur. Ceram. Soc. 35 (2015) 4411–4422. https://doi.org/10.1016/j.jeurceramsoc.2015.08.027.

[28] L.M. BRESCIANI, A. MANES, M. GIGLIO, An analytical model for ballistic impacts against ceramic tiles, Ceram. Int. 44 (2018) 21249–21261. https://doi.org/10.1016/j.ceramint.2018.08.172.

[29] K. AKELLA, Studies for Improved Damage Tolerance of Ceramics Against Ballistic Impact Using Layers, Procedia Eng. 173 (2017) 244–250. https://doi.org/10.1016/j.proeng.2016.12.006.

[30] C.E.J. DANCER, J.N.F. SPAWTON, S. FALCO, N. PETRINIC, R.I. TODD, Characterisation of damage mechanisms in oxide ceramics indented at dynamic and quasi-static strain rates, J. Eur. Ceram. Soc. 39 (2019) 4936–4945. https://doi.org/10.1016/j.jeurceramsoc.2019.06.054.

[31] A. BALASUBRAMANIAN, B. LEVINE, AND A. VENKATARAMANI, DTN Routing as a Resource Allocation Problem, In Proceedings of the Conference on Applications, Technologies, Architectures, and Protocols for Computer Communications, 2007, pages 373–384, New York, NY, USA. ACM.

[32] A. EFTEKHARI, B. MOVAHEDI, G. DINI, M. MILANI, Fabrication and microstructural characterization of the novel optical ceramic consisting of □-Al2O3@amorphous alumina nanocomposite core/shell structure, J. Eur. Ceram. Soc. 38 (2018) 3297–3304. https://doi.org/10.1016/j.jeurceramsoc.2018.02.038.

[33] S. LAMOURI, M. HAMIDOUCHE, N. BOUAOUADJA, H. BELHOUCHET, V. GARNIER, G. FANTOZZI, J.F. TRELKAT, Control of the □-alumina to □-alumina phase transformation for an optimized alumina densification, Bul. La Soc. Esp. Cer. y Vidr. 56 (2017) 47–54. https://doi.org/10.1016/j.bsecv.2016.10.001.

[34] P. MILAK, F.D. MINATTO, C. FALLER, A. DE NONI, O.R. KLEGUES MONTEDO, The influence of dopants in the grain size of alumina - A review, Mater. Sci. Forum. 820 (2015) 280–284. https://doi.org/10.4028/www.scientific.net/MSF.820.280.

[35] A.V. GOMES, L.H.L. LOURO, C.R.C COSTA, Ballistic behavior of alumina with niobia additions. Journal de Physique IV (Proceedings), [S.L.], v. 134, p. 1009-1014, 26 jul. 2006. Http://dx.doi.org/10.1051/jp4:2006134154.

[36] W. TRINDADE, M.H.P. SILVA, A.V. GOMES, J.B. CAMPOS, L.H.L. LOURO, Processing and Properties of Niobia-Doped Alumina Sintered at 1400oC. Mat. Sci. For. 798 (2014) 665-670. Http://dx.doi.org/10.4028/www.scientific.net/msf.798-799.665.

[37] J.L. SANTOS, R.L.S.B. MARÇAL, P.R.R. JESUS, A.V. GOMES, E.P. LIMA, S.N. MONTEIRO, J.B. CAMPOS, L.H.L. LOURO, Effect of LiF as Sintering Agent on the Densification and Phase Formation in Al2O3-4 Wt Pct Nb2O5 Ceramic Compound. Met. Mat. Trans. A 48 (2017) 10 4432-4440. Http://dx.doi.org/10.1007/s11661-017-4271-y.

[38] P.H.P.M. SILVEIRA, P.R.R. JESUS, M.P. RIBEIRO, S.N. MONTEIRO, J.C.S. OLIVEIRA, A.V. GOMES, Sintering Behavior of AL2O3 Ceramics Doped with Pre-Sintered NB2O5 and LiF, Mat. Sci. For. 1012 (2020) 190-195. Http://dx.doi.org/10.4028/www.scientific.net/msf.1012.190.

[39] NBR 16661:2017. Material refratário denso conformado – determinação de volume aparente, volume aparente da parte sólida, densidade da massa aparente, densidade aparente da parte sólida, porosidade aparente e absorção. ABNT. 2ª edição; 2017

[40] J.I. Im, Y.J. Yook, FE Analysis of Alumina Green Body Density for Pressure Compaction Process. J. of the Kor. Cer. Soc. 43(12) (2006) 859-864. Http://dx.doi.org/10.4191/kcers.2006.43.12.859.

[41] W. TRINDADE, M.H.P. SILVA, A.V. GOMES, C.F.M. CHAGAS, L.H.L. LOURO, J.B. CAMPOS, Comparative Study of Solid-Phase and Liquid-Phase Assisted Sintering of Nb2O5-Doped Alumina, Mat. Sci. For. 798-799 (2014) 691-695. Http://dx.doi.org/10.4028/www.scientific.net/msf.798-799.691.

[42] W. TRINDADE, M.H.P. SILVA, A.V. GOMES, C.F.M. CHAGAS, L.H.L. LOURO, Effect of Milling Medium on Alumina Additivated with Niobia. Mat. Sci. For. 798-799 (2014) 677-681. Http://dx.doi.org/10.4028/www.scientific.net/msf.798-799.677.

[43] R.M. GERMAN, P. SURI, S.J. PARK, REVIEW: liquid phase sintering. J. Mat. Sci, [S.L.], v44(1) (2009) 1-39. Http://dx.doi.org/10.1007/s10853-008-3008-0.

[44] F. KONG, L. LV, J. WANG, G. JIAO, S. TAO, Z. HAN, Y. FANG; B. QIAN, X. JIANG, Graphite modified AlNbO 4 with enhanced lithium — Ion storage behaviors and its electrochemical mechanism. Mat. Res. Bul. 97 (2018) 405-410. Http://dx.doi.org/10.1016/j.materresbull.2017.09.034.

[45] L.O. SVAASAND, M. ERIKSRUD, G. NAKKEN, A.P. Grande, Solid-solution range of LiNbO3. J. of Crys. Grow. 22(3) (1974) 230-232. Http://dx.doi.org/10.1016/0022-0248(74)90099-2.

[46] Z. LI, F. HUANG, X. FENG, A. YAN, H. DONG, M. HU, Q. LI, Tunable band alignment in two-phase--coexistence Nb3O7F nanocrystals with enhanced light harvesting and photocatalytic performance, Nanotech. 29(22) (2018) 225605. Http://dx.doi.org/10.1088/1361-6528/aab68e.

[47] P. MILAK, F.D. MINATTO, C. FALLER, A. NONI-JUNIOR, O.R.K. MONTEDO, The Influence of Dopants in the Grain Size of Alumina - A Review, Mat. Sci. For. 820 (2015) 280-284. Http://dx.doi.org/10.4028/www.scientific.net/msf.820.280.

[48] K. BODILOVÁ, D. GALUSEK, P.; VANČÁREK, V. POUCHLÝ, K. MACA, Grain growth suppression in alumina via doping and two-step sintering, Cer. Int. 41(9) (2015) 11975-11983. Http://dx.doi.org/10.1016/j.ceramint.2015.05.162.